Adaptive Noise Reduction toward Low-dose Computed Tomography

Hongbing Lu[*ad], Xiang Li[a], Lihong Li[a], Dongqin Chen[b], Yuxiang Xing[a], Jiang Hsieh[c] and Zhengrong Liang[**a]

[a]Department of Radiology, State University of New York, Stony Brook, NY USA 11794
[b]Viatronix Inc, 25 East Loop Rd., Stony Brook, NY USA 11790
[c]Applied Science Laboratory, GE Medical Systems, Milwaukee, WI USA 53201
[d]Department of Computer Application, Fourth Military Medical University, Xi'an, China 710032

ABSTRACT

An efficient noise treatment scheme has been developed to achieve low-dose CT diagnosis based on currently available CT hardware and image reconstruction technologies. The scheme proposed includes two main parts: filtering in sinogram domain and smoothing in image domain. The acquired projection sinograms were first treated by our previously proposed Karhunen-Loeve (K-L) domain penalized weighted least-square (PWLS) filtering, which fully utilizes the prior statistical noise property and three-dimensional (3D) spatial information for an accurate restoration of the low-dose projections. To treat the streak artifacts due to photon starvation, we also incorporated an adaptive filtering into our PWLS framework, which selectively smoothes those channels contributing most to the streak artifacts. After the sinogram filtering, the image was reconstructed by the conventional filtered backprojection (FBP) method. The image is assumed as piecewise regions each has a unique texture. Therefore, an edge-preserving smoothing (EPS) with locally-adaptive parameters to the noise variation was applied for further noise reduction in image domain. Experimental phantom projections acquired by a GE spiral computed tomography (CT) scanner under 10 mAs tube current were used to evaluate the proposed smoothing scheme. The reconstructed imaged demonstrated that the smoothing scheme with appropriate control parameters provides a significant improvement on noise suppression without sacrificing the spatial resolution.

Keywords: Noise reduction, nonstationary noise, dose reduction, computed tomography, adaptive filtering, edge-preserving smoothing, streak artifacts.

1. INTRODUCTION

Currently available spiral/helical computed tomography (CT) technologies have demonstrated the potential for four-dimensional (4D) dynamic imaging at less than 1 mm spatial resolution. In addition, many recent investigations have demonstrated that CT can be considered to be a candidate technique for mass screening applications, such as screening of the lung nodules and colonic polyps, 3D mammography, and etc[1]. However, a major limitation for its clinical applications is associated with the high radiation exposure, especially for women and children. The only solution is to deliver less x-rays to the body or equivalently lower down the electric current of the x-ray tube (or mA) in data acquisition protocols. Unfortunately, the resulting images have very noisy appearance with unacceptably low image quality, making the diagnosis very difficult. Therefore, an efficient noise treatment is a necessary prerequisite to reduce radiation dosage and make the low-dose CT diagnosis feasible. Parallel to the great effort devoted to improve the hardware performance of CT/ECT (emission CT) scanners, software approaches by modeling the noise properties and then removing the noise from the CT/ECT data, both before and after image is reconstructed, can be a more cost-effective means towards low-dose CT modality. Although several noise investigations have been made in CT field in the last two decades, they focused on the noise power spectrum properties and did not present a strategy to handle the projection data noise for an improved image reconstruction [2, 3]. Many other investigations were taken to smooth the image noise after or post reconstruction. For example, Sauer and Liu [4] attempted to smooth the noise of the reconstructed CT images by a non-stationary filter, which was designed based on the local noise property on the images. Two studies on the projection data were reported in [5, 6]. Hsieh [5] employed an adaptive trimmed mean filter to reduce the streak artifacts due to photon starvation, while Demirkaya [6] designed a non-linear anisotropic diffusion filter based

* luhb@fmmu.edu.cn; phone 86 29 3374-840; fax 86 29 3374-837; http://fmmu.edu.cn; ** jzl@clio.mil.sunysb.edu; phone 1 631 444-7837; fax 1 631 444-6450; http://www.mil.sunysb.edu/micl/.

Medical Imaging 2003: Physics of Medical Imaging, M. J. Yaffe, L. E. Antonuk, Editors, Proceedings of SPIE Vol. 5030 (2003) © 2003 SPIE · 1605-7422/03/$15.00

on a Gaussian statistics with the variance proportional to the datum itself. All the previous filters were based on some kinds of *ad hoc* assumptions, lacking the ground truth.

To achieve low-dose CT diagnosis based on currently available CT hardware and image reconstruction technologies, we previously analysed the noise properties of acquired data for the ground truth and incorporated the modeled noise proporties into a statistical framework for an accurate treatment on the low-dose data noise[7-11]. In this study, we further demostrated the usage of our efficient filtering algorithms, as a preprocessing means in both sinogram and image domains, to reduce any noise-related artifacts for low-dose CT modality.

2. METHODS

2.1. Description of the adaptive noise treatment scheme

Our noise treatment scheme for low-dose CT includes two parts: adaptive filtering in sinogram space and adaptive smoothing in image domain. As shown in Figure 1, the acquired projection sinograms are first treated by our previously proposed Karhunen-Loeve (K-L) domain penalized weighted least-square (PWLS) filtering, which is based on the nonlinear noise property or "ground truth" of the low-dose CT projections acquired from phantom experiments. To mitigate the streak artifacts, an adaptive filtering is incorporated into the PWLS framework, which selectively smoothes those channels contributing most to the streak artifacts. After the sinogram filtering, the image is reconstructed by the conventional filtered backprojection (FBP) method. The image is assumed as piecewise regions each has a unique texture. Therefore, an edge-preserving smoothing (EPS) with locally-adaptive parameters to the noise variation is applied for further noise reduction in the image domain.

In the following subsections, we will describe our adaptive noise treatment scheme in detail.

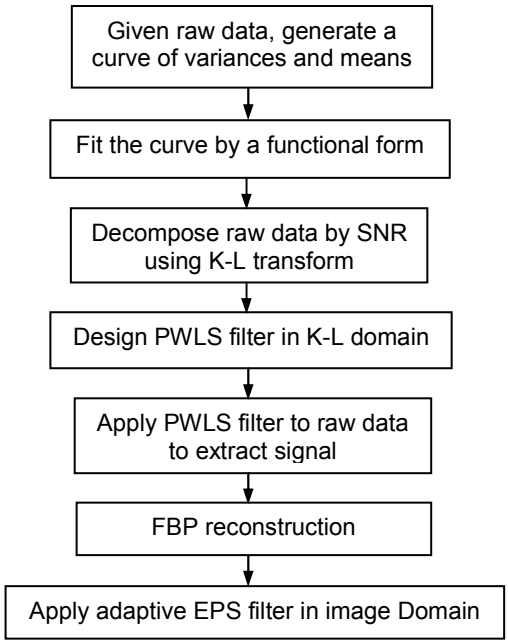

Figure 1. Flow chart of our noise treatment scheme proposed.

2.2. K-L domain penalized weighted least-square filtering in sinogram space

In sinogram domain, as we know, the projection data acquired for image reconstruction of low-dose CT are degraded by many factors, such as system calibration for the geometrical effect and the non-uniformity of x-ray flux, and log transform to satisfy the Radon transform for image reconstruction. These factors complicate noise analysis on the projection data and render a very challenging task for noise reduction. To achieve accurate noise treatment in sinogram space, we previously investigated the noise properties of the projection data by analyzing repeatedly acquired

experimental phantom data sets [9, 11]. The statistical analysis shows that the noise can be regarded as normally distributed with a nonlinear signal-dependent variance. Given the Gaussian distribution and the nonlinear mean-variance curve, the PWLS principle could be an optimal choice to fully utilize the obtained noise properties [12-16]. Another modified K-L transform decomposes the entire data information into components with different signal-to-noise (SNR) properties [17-20], resulting in a PWLS smoothing in the K-L domain. In our noise treatment scheme, the projection sinograms are first treated by the K-L domain PWLS smoothing [11]. By selecting an appropriate number of neighboring sinogram slices, it fully utilizes the prior statistical knowledge and 3D spatial information for an accurate restoration of the noisy projections.

Another problem induced by low-dose CT is the severe streak artifacts due to photon starvation, as shown in the middle of Figure 3. The previous analysis from Hsieh [5] clearly indicates that the logarithm operation has played a significant role in the amplication of the noise when the detector signal is low. To treat the streak artifacts, an adaptive filtering is incorporated into our PWLS framework based on the above physical analysis. It selectively smoothes those channels contributing most to the streak artifacts. The degree of smoothing in the selected channels varies based on the noise level of the signal. It should be noted that the streak artifacts in reconstructed images of low mA protocols render a very challenging problem for post-reconstruction noise reduction means, as shown in Figure 3, while our strategy in sinogram space avoids this problem.

After filtering, the sinograms are reconstructed by the conventional FBP method, which has been optimized for many years for accuracy and efficiency.

2.3. Adaptive edge-preserving smoothing in image space

It is well known that any noise reduction means without resolution preservation built in will have a cost of more or less resolution loss. In order to minimize the resolution loss during our noise-reduction process, we imposed an edge-preservation strategy in the process. After sinogram filtering, the reconstructed images can be assumed as piecewise regions each has a unique texture property. Therefore, in image domain, edge-preserving smoothing (EPS) is of potential interest for further noise reduction. It simultaneously smoothes the noise and preserves the edges by selectively local average without crossing the edges [21-28]. To find an EPS algorithm appropriate for the smoothing task in the image space, we performed a comparison study by numerical simulations with different kind of noise at different noise levels, as shown in Figure 2. Among the EPS algorithms tested, the non-linear Gaussian filter (NLGF) chains [21, 23], a representative algorithm of the group of EPS, outperforms other algorithms and smoothes the image noise without destroying fine details and coarser structures. In this study, we adapted a similar NLGC chain as that of Aurich and Weule proposed [21] and, therefore, the same notations will be used throughout this paper.

For an image with value *f(p)* at pixel *p*, a nonlinear Gaussian filtering operation is defined by [21]:

$$G_{\sigma_x,\sigma_z} f(p) = f(p) + \eta \cdot \tfrac{1}{N_p} \sum_{q \in P} g_{\sigma_x}(\|q-p\|) g_{\sigma_z}(f(q)-f(p)) \cdot (f(q)-f(p)) \qquad (1)$$

$$\text{with} \quad g_\sigma(t) = \exp(\frac{-t^2}{2\sigma^2}) \quad \text{and} \quad N_p = \sum_{q \in P} g_{\sigma_x}(\|q-p\|) g_{\sigma_z}(f(q)-f(p)).$$

where σ_x and σ_z are smoothing parameters measuring the width of $g_{\sigma x}$ and $g_{\sigma z}$, respectively. Notation P covers the neighborhood of pixel p and η is chosen to provide numerical stability of the approximation.

For sufficient smoothing, several filtering steps with different parameters are usually performed, which is therefore called NLGF chains. Formally it may be written by the form of

$$G^{\sigma_{xn},\sigma_{zn}} \circ \cdots \circ G^{\sigma_{x1},\sigma_{z1}} F. \qquad (2)$$

In addition to a better smoothing effect, the NLGF chain has several important advantages for our purpose. It is numerically robust (choice of the parameters is not critical). It is much faster than robust statistics estimation smoothing. A chain of three to five filters with suitable parameters is enough to differentiate random noise from intrinsic information (structure) in an image.

However, in some clinical cases, we couldn't acquire projection data directly due to mechanic inaccessibility. Though EPS can still be applied directly in this situation, it is sub-optimal because the EPS methods usually assign a uniform standard deviation to all pixels without considering the noise spatial variation in the reconstructed image (due to

nonstationary noise in the projection domain). For a better treatment of the non-uniform variation of the noise existed in CT reconstructed images, we analyzed the noise properties of FBP reconstruction procedure and developed an adaptive edge-preserving smoothing method with parameters locally adaptive to the raw data and noise variation.

Under an assumption of uncorrelated noise, the variance of the distribution between pixel p and q is

$$\sigma_{p,q}^{\ 2} = \sigma_p^{\ 2} + \sigma_q^{\ 2}$$

where σ_p and σ_q are the standard deviation of pixel p and q, respectively.

Choosing a "robust scale" [21] for rejection of edges for each pair of the neighboring pixels p and q in terms of the population standard deviation $\sigma_{p,q}$, the smoothing parameter σ_z above can be expressed as

$$\begin{aligned} \sigma_{z_{p,q}} &= \omega \cdot \sigma_{p,q} \\ &= \omega \cdot \sqrt{\sigma_p^{\ 2} + \sigma_q^{\ 2}} \end{aligned} \tag{3}$$

which is spatially variant and locally adaptive to the noise variation. Notation ω is a normalization weight and can be determined by the filtering function. Considering Eqs.(1) and (3), our proposed adaptive EPS takes the noise properties into account, as well as the spatial information.

3. EXPERIMENTAL RESULTS

The effectiveness of our filtering system, as a preprocessing means in both sinogram and image domains for reducing noise as a low-dose CT modality, has been evaluated by both numerical and experimental phantom datastes, as well as patient studies. To find an EPS algorithm appropriate for the smoothing task in the image space, we performed a comparison study by numerical simulations with different kind of noise at different noise levels. The EPS algorithms used for comparison are (1) the anisotropic diffusion filter (ADG) with Gaussian kernal from Perona and Malik [24], 92) the modified well-posed anisotropic diffusion filter (ADM) from You and Xu [28], (3) the noise-adjusted anisotropic diffusion filter (NAAD) proposed by Samsonov and Johnson [30], and (4) the non-linear Gaussian filter chains (NLGC) [21]. The digital Shepp-Logan phantom with four different activity levels was used for numerical simulations. Figure 2 shows the results for images contaminated by different kinds of noise at different noise levels. The noise added to the top row of Figure 2 was Gaussian distributed with SNR equal to 1.15, while noise added to the middle row had a lower SNR equal to 0.5. Here SNR is defined as the image contrast divided by the standard deviation of the added noise. As mentioned before, the noise in the reconstructed images is usually spatially-variant due to the nonstationary property in the projection domain. To demonstrate the smoothing effect of EPS algorithms on nonstationary noise, Poisson noise was added into the bottom row of Figure 2. Comparing the performance of the NLGC, ADG, ADM, and NAAD filters as shown in Figure 2, it's clearly seen that NLGC filter significantly outperforms other edge-preserving smoothing algorithms, for images with either Gaussian or Poisson noise, at different noise levels. It provides significant improvement on noise reduction without destroying fine details and coarser structures. Therefore, we incorporated the NLGC filtering into our noise reduction scheme and developed our adaptive edge-preserving smoothing based on the NLGC framework.

Though the NLGC filter shows excellent performance in the numerical simulations, it needs further verification for patient studies. A patient dataset was acquired by a GE spiral CT scanner located at SUNY-SB university hospital. Besides a normal scan performed at a routine clinical dosage (150 mA), an additional scan from the same patient was acquired at a much lower tube current, i.e. 20 mA. One slice extracted from the same position of the two CT datasets is shown, respectively, on the left and in the middle of Figure 3. Severe streak artifacts are observed clearly in the low-dose CT image due to photon starvation, see the middle of Figure 3. The right figure shows the result after our NLGC filtering with initial parameters σ_x set to 0.82 and σ_z to 160. It demonstrates that our NLGC filtering works pretty well in relatively uniform regions, but is not very efficient in regions with severe streak artifacts. It should be noted that the streak artifacts in the reconstructed images of low mA protocols render a very challenging problem for any post-reconstruction noise reduction means. An efficient sinogram filtering with appropriate treatment on the streak artifacts before image reconstruction is quite critical to the final low-dose CT image quality. That is the reason why we incorporate an adaptive filtering for removal of the streak artifacts into our PWLS framework in the sinogram space.

Here we didn't show the effect of our K-L domain PWLS filtering on the patient dataset because of the inaccessibility of projection data from the hospital CT scanner. This will be our next research task and is under progress.

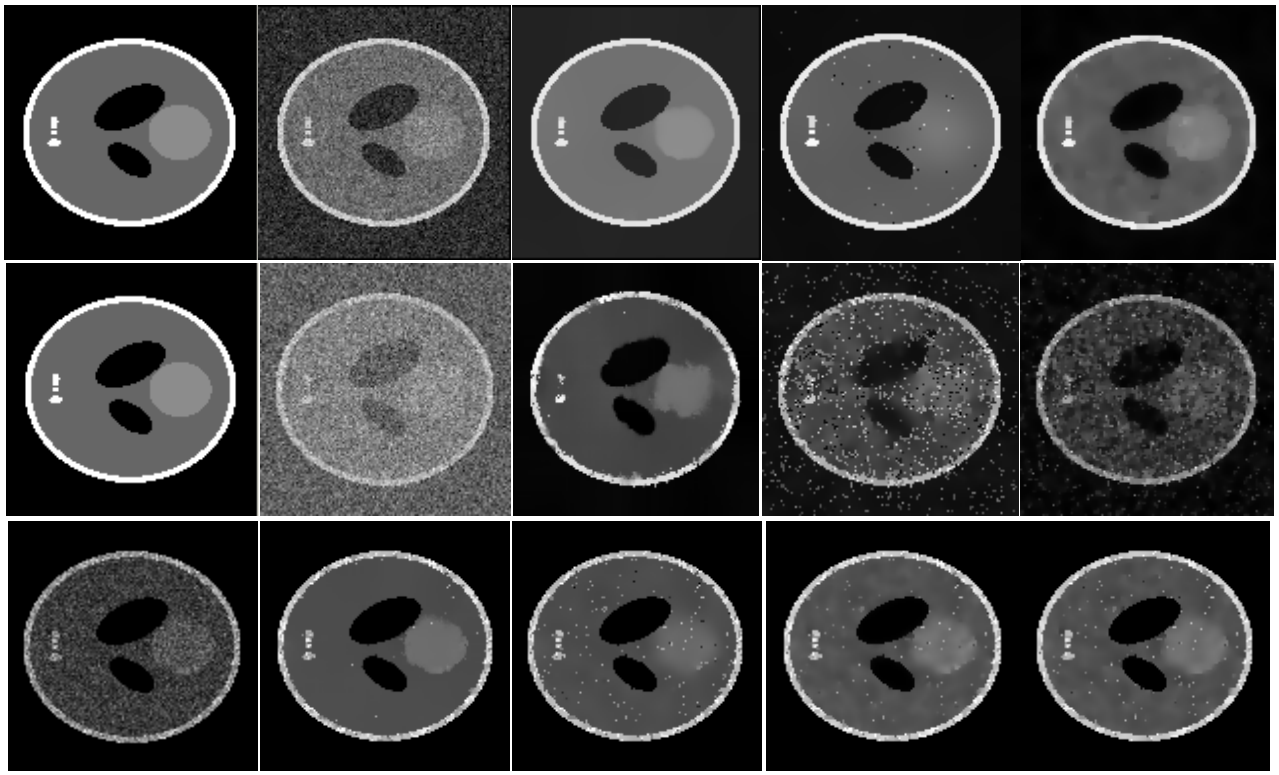

Figure 2. Comparison study on the performance of different EPS algorithms by numerical simulations. Top, Gaussian noise, SNR=1.15, from left to right -- Phantom, noisy image, improved results by NLGC, ADG, ADM, respectively. Middle, Gaussian noise, SNR=0.5, from left to right -- Phantom, noisy image, improved results by NLGC, ADG, ADM, respectively. Bottom, Poisson noise, from left to right -- noisy image, improved results by NLGC, ADG ADM, NAAD, respectively.

Figure 3. Patient study on the performance of NLGC algorithm. From left to right -- CT slices acquired at normal clinical dosage (150 mA), acquired at lower dosage (20 mA), and improved image smoothed by NLGC (σ_x=*0.82,* σ_z =160).

To evaluate the proposed noise reduction scheme, we performed a pilot study on noise modeling and treatment for noisy CT projection data using a GE high-speed spiral four detector band CT scanner and a cylinder phantom. The phantom is the GE Quality Assurance Phantom of a cylindrical tank with 20 cm diameter and Plexglass wall. It has a Plexglass square volume in the center. Water was filled between the central part and the wall. For details, see the left-up picture of Figure 4, where the small lines and strips inside the Plexglass volume were filled with air. The phantom was positioned in the FOV center of a GE four-detector band spiral CT scanner. The detector rotated 19 times around the phantom in a cine mode (i.e., the table remained at one location), resulting in 19 sets of projection datasets each with

984 views evenly distributed over 360 degrees. The acquisition tube current was 10mAs, with a fixed kVp value of 120. The reconstructed slices obtained using different filtering approaches are shown in the Figure 4.

Compared to the gold standard reconstruction (from the summation of 19 datasets, the top left of Figure 4) and the noisy reconstruction without treatment (from a single dataset, the top middle of Figure 4), all the noise treatment methodologies provided improvement on noise suppression. After a non-iterative lest-square minimization, in the K-L domain, on the same single projection dataset above, an inverse K-L transform was performed. The resulted image is shown in the top right of Figure 4. When the reconstructed slice was further treated by the NLGC smoothing in the image domain, a further improvement is clearly seen toward the gold standard, as shown by the bottom left of Figure 4. The improved results with only filtering in the image domain are also demonstrated in Figure 4 (bottom middle and right), but they are not comparable to our result of bottom left. Although the performance of the adaptive EPS outperformed that of the NLGC, it is quite sub-optimal as compared to the result obtained by K-L domain PWLS plus NLGC (by our means). This suggests that appropriate filtering before reconstruction is critical to the final image quality, as we mentioned above. The reconstructed results shown in Figure 4 have demonstrated that the proposed scheme with appropriate parameter controls provides a significant improvement on noise suppression without sacrificing the spatial resolution.

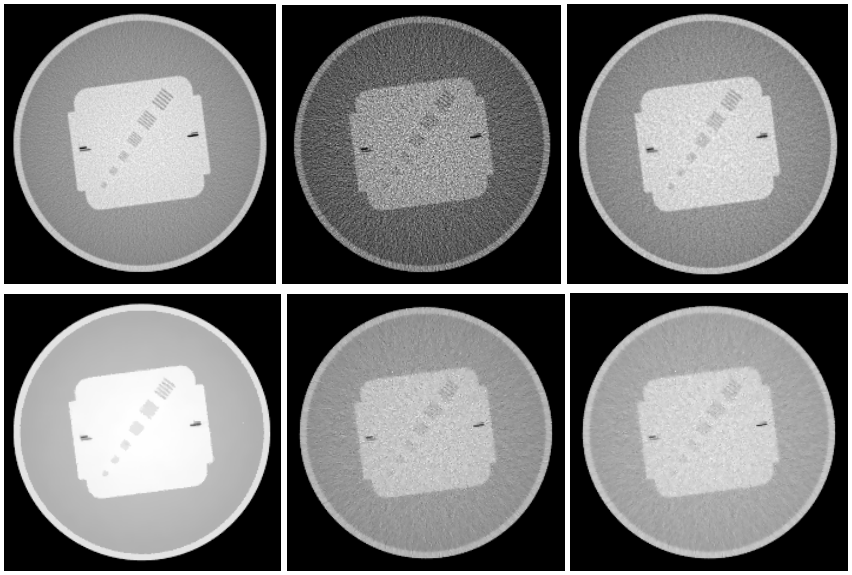

Figure 4. Comparison of the reconstructed CT images using different filtering strategies. Upper, from left to right – "noise-free" or gold stand image, noisy image from a single dataset (without noise treatment), improved result by the K-L domain PWLS smoothing in the sinogram space only. Bottom -- improved results by the K-L domain PWLS+NLGC; the NLGC in the image space only; and the adaptive EPS in the image space only.

4. DISCUSSION AND CONCLUSION

Our noise treatment scheme provides an efficient means towards low-dose CT modality. The innovation resides in the integration of fully available information into a well-established framework for an accurate handling of the problem. It accounts for not only the prior knowledge of the noise properties, but also the 3D spatial information. Therefore, more accurate treatment of nonstationary noise can be achieved for low-dose CT/ECT applications. This software module of noise treatment is quantitatively accurate and computationally efficient. It costs nothing, except for a few minutes of computing time, but it achieves minimal radiation for both CT and ECT. Therefore, it will broaden the use of these modalities, especially for mass screening application. Low-dose experimental results demonstrate that the proposed system with appropriate control parameters provides a significant improvement on noise suppression without sacrificing the spatial resolution.

The noise treatment methodologies proposed in sinogram domain are analytical or non-iterative and therefore theoretically attractive. The whole scheme described here is based on the noise modeling and the incorporating of the modeled noise properties (or "ground truth", not *ad hoc* assumptions) into a mathematically or statistically rigorous framework. They treat the noise both in the data space and image space and fully take the advantages of the well-established, fast, accurate FBP reconstruction techniques, which have been developed in the past decades in the CT field. Furthermore, they are insensitive to the selection of the parameters and are robust in use.

Further evaluation of the established noise treatment methodologies by multiple phantom experiments with different mA values in the range from 10 to 300, two anthropomorphic (head and torso) phantoms, given kVp value of 120 (the electric voltage across the x-ray tube) is under investigation.

ACKNOWLEDGEMENT

This work was supported in part by the National Heart, Lung and Blood Institute under Grant No. HL54166 and the National Natural Science Foundation of China under Grant No. 30170278. The authors would like to appreciate Dr. Mark Wax for providing the patient data.

REFERENCES

1. G.F. Rust, V. Aurich and M. Reiser (2002), "Noise/dose reduction and image improvements in screening virtual colonoscopy with tube currents of 20 mAs with nonlinear Gaussian filter chains", *SPIE Medical Imaging*, **4683**: 186-197.
2. M.F. Kijewski and P.F. Judy (1987), "The noise power spectrum of CT images", *Physics in Medicine and Biology*, **32**: 565-575.
3. S.J. Riederer, N.J. Pelc and D.A. Chesler (1978), "The noise power spectrum in computed x-ray tomography", *Physics in Medicine and Biology*, **23**: 446-454.
4. K. Sauer and B. Liu (1991), "Non-stationary filtering of transmission tomograms in high photon counting noise", *IEEE Trans. Med. Imaging*, **10**: 445-452.
5. J. Hsieh (1998), "Adaptive streak artifacts reduction in computed tomography resulting from excessive x-ray photon noise", *Medical Physics*, **25**: 2139-2147.
6. K. Demirkaya (2001), "Reduction of noise and image artifacts in computed tomography by nonlinear filtration of the projection images", *SPIE Medical Imaging*, **4322**: 917-923.
7. H. Lu, Z. Liang, D. Chen, and *et al.* (2001), "A combined transformation of ordering SPECT sinograms for signal extraction from measurements with Poisson noise", *SPIE Medical Imaging*, **4322**: 943-951.
8. H. Lu, I. Hsiao, X. Li and Z. Liang (2001), "Spatial resolution uniformity of K-L transform on projection data along different directions for SPECT imaging", *Journal of Nuclear Medicine*, **42**: 200P.
9. H. Lu, I-T. Hsiao, X. Li, and Z. Liang (2001), "Noise properties of low-dose CT projections and noise treatment by scale transformations", *Conference Record of IEEE NSS and MIC*, in CD-ROM.
10. H Lu, Z. Liang, D. Chen, and *et al*. (2001), "A combined transformation of ordering SPECT sinograms for signal extraction from measurements with Poisson noise", *SPIE Medical Imaging,* **4322**: 1431-1438.
11. H. Lu, X. Li, I-T. Hsiao, and Z. Liang (2002), "Analytical treatment of noise for low-dose CT projection data by penalized weighted least-square smoothing in the K-L domain", *SPIE Medical Imaging*, **4682**: 146-152.
12. J.A. Fessler (1994), "Penalized weighted least-squares image reconstruction for positron emission tomography", *IEEE Trans. Med. Imaging*, **13**: 290-300.
13. J.A. Fessler (1993), "Tomographic reconstruction using information-weighted spline smoothing", in Info. Proc. In Med. Imag., H.H. Barrett and A.F.Gmitro, Eds. Heidelberg: Spring-Verlag, pp.372-386.
14. J.A. Fessler, and W.L. Rogers (1996), "Spatial resolution properties of penalized-likelihood image reconstruction: space-invariant tomographs", *IEEE Trans. Image Processing*, **5**: 1346-1358.
15. J.A. Fessler (1991), "Nonparametric fixed-interval smoothing with vector splines", *IEEE Trans. Sig. Proc*., **39**: 852-859.
16. P.J. La Rivière and Xiaochuan Pan (2000), "Nonparametric regression sinogram smoothing using a roughness-penalized Poisson likelihood objective function", *IEEE Trans. Med. Imaging*, **19**: 773-786.
17. B.R. Hunt, and O. Kübler (1984), "Karhunen-Loeve multi-spectral image restoration, part I: theory*", IEEE Trans. Acoustics, Speech, and Signal Processing*, **ASSP-32**: 592-600.

18. J.B. Lee, A.S. Woodyatt, and M. Berman (1990), "Enhancement of high spectral resolution remote-sensing data by a noise-adjusted principal components transform", *IEEE Trans. Geosci. Remote Sensing,* **28**: 295-304.
19. M.N. Wernick, E.J. Infusino, and C.M. Kao (1997), "Fast optimal pre-reconstruction filters for dynamic PET", *Conference Record of the IEEE NSS and MIC*, in CD-ROM.
20. M.N. Wernick, E.J. Infusino, and M. Milosevic (1999), "Fast Spatio-temporal image reconstruction for dynamic PET", *IEEE Trans. Med. Imaging*, **18**: 185-195.
21. V. Aurich and J. Weule (1995), "Non-linear Gaussian filters performing edge preserving diffusion", in *Proceedings 17. DAGM Symposium über Mustererkennung,* pp. 538-545, Springer.
22. C-K. Chu, I.K. Glad, F. Godtliebsen, and *et al*. (1998), "Edge-preserving smoothers for image processing", *J. of the American Statistical Association*, **93**(442): 526-541.
23. K. Kitamura, H. Iida, M. Shidahara, and *et al*. (2000), "Noise reduction in PET attenuation correction using non-linear Gaussian filters", *IEEE Trans. Nucl. Science,* **47**(3): 994-999.
24. P. Perona and J. Malik (1990), "Scale-space and edge detection using anisotropic diffusion", *IEEE Trans. Pattern Anal. And Machine Intelligence*, **12**(7): 629-639.
25. J. Polzehl and V.G. Spokoiny (2000), "Adaptive weights smoothing with applications to image restoration", *J. R. Statist. Soc. B*, **62**, Part2: 335-354.
26. H. Rue, C-K. Chu, F. Godtliebsen, and *et al*. (2002), "M-smoother with local linear fit", *Journal of Nonparametric Statistics*, **14**: 155-168.
27. G. Winkler, V. Aurich, K. Hahn, and *et al*. (1999), "Noise reduction in images: some recent edge-preserving methods", *Pattern Recognition and Image Analysis*, **9**(4): 749-766.
28. Y-L. You, W. Xu, A. Tannenbaum, and *et al*. (1996), "Behavioral analysis of anisotropic diffusion in image processing", *IEEE Trans. Image Processing*, **5**(11): 1539-1551.
29. D.F. Yu and J.A. Fessler (2000), "Three-dimensional non-local edge-preserving regularization for PET transmission reconstruction", *Conference Record of the IEEE NSS and MIC*, in CD-ROM.